Available online at www.sciencedirect.com
SCIENCE DIRECT®
Journal of Power Sources 129 (2004) 368–378
JOURNAL OF POWER SOURCES
www.elsevier.com/locate/jpowsour

HEV battery heating using AC currents

T.A. Stuart [a], A. Hande [b,*]

[a] *University of Toledo, Toledo, OH, USA*
[b] *Lake Superior State University, Sault Ste. Marie, MI, USA*

Received 29 September 2003; accepted 21 October 2003

Abstract

A unique method has been developed for internally heating hybrid electric vehicle (HEV) batteries at cold temperatures using alternating current (AC). The poor performance of these batteries in cold climates is of major concern because they suffer a huge loss in capacity. Another symptom of this low performance is a dramatic increase in the series resistance of the battery, R_B, as the temperature drops. Experiments were performed with both low and high frequency heaters, and several tests were conducted on both lead acid and nickel metal hydride (NiMH) batteries at different AC amplitudes, states of charge (SOCs) and cold temperatures. Low frequency 60 Hz heating was first tested on several different 38 Ah lead acid batteries. The feasibility of using high frequency heating was then tested using a 10–20 kHz inverter on a pack of 6.5 Ah nickel metal hydride (NiMH) batteries. A technique also was developed to estimate the internal battery temperature, T_{bat}, by measuring the battery source resistance, R_B.

Keywords: Hybrid electric vehicle; Alternating current; Nickel metal hydride

1. Introduction

Hybrid electric vehicles (HEVs) make use of alternate energy sources such as electrochemical secondary batteries, flywheels and ultracapacitors for propulsion. However, at present virtually all of these vehicles use large packs of batteries connected in series. These batteries are perishable products and deteriorate as a result of the chemical action that proceeds during usage and storage. The cell design, temperature, and length of usage/storage are a few factors that affect the life or charge retention of these batteries [1]. Some of the more popular versions used in today's HEVs, include lead acid, NiMH and lithium-ion.

Every battery has a rated capacity which indicates the maximum charge that can be put into it. This is known as the full charge capacity. The actual capacity of a battery indicates the actual charge it possesses. Both these capacities are usually defined in ampere–hours (Ah; instead of coulombs) and can be calculated from the following equation:

$$\text{battery capacity}\,(Q) = {}_t\int i\,\mathrm{d}t \tag{1}$$

Therefore, battery capacity indicates the amount of charge it is capable of storing and delivering to an electrical load. This also depends on the rate of discharge, and the higher the rate of discharge, the lower the usable battery capacity. The actual capacity is sometimes referred to, on a percentage basis, as the state of charge (SOC). SOC is defined as

$$\text{SOC} = \frac{\text{actual } Q}{\text{maximum } Q} \times 100\% \tag{2}$$

It is well known that Q also decreases with a decrease in ambient temperature. The degree of the ambient temperature effect on the capacity depends upon the type and quality of the electrolyte and the SOC. This decrease in battery capacity at low temperatures occurs because the viscosity of the electrolyte increases, and in some cases the electrolyte can actually freeze. This limits the flow of current from one electrode to the other, and the battery resistance increases. At very low temperatures this effect can be dramatic, and the electrolyte needs to be warmed so that the vehicle will operate satisfactorily.

At cold temperatures such as those below 0 °C, battery charge and discharge become increasingly difficult. Fig. 1 shows a simplified model that can be used to explain the problem for most types of batteries.

The model consists of three parts:

1. An ideal voltage source, V_0, that represents the charge storage mechanism.

* Corresponding author. Tel.: +1-906-635-2598; fax: +1-906-635-6663.
E-mail address: ahande@lssu.edu (A. Hande).

0378-7753/$ – see front matter © 2003 Elsevier B.V. All rights reserved.
doi:10.1016/j.jpowsour.2003.10.014

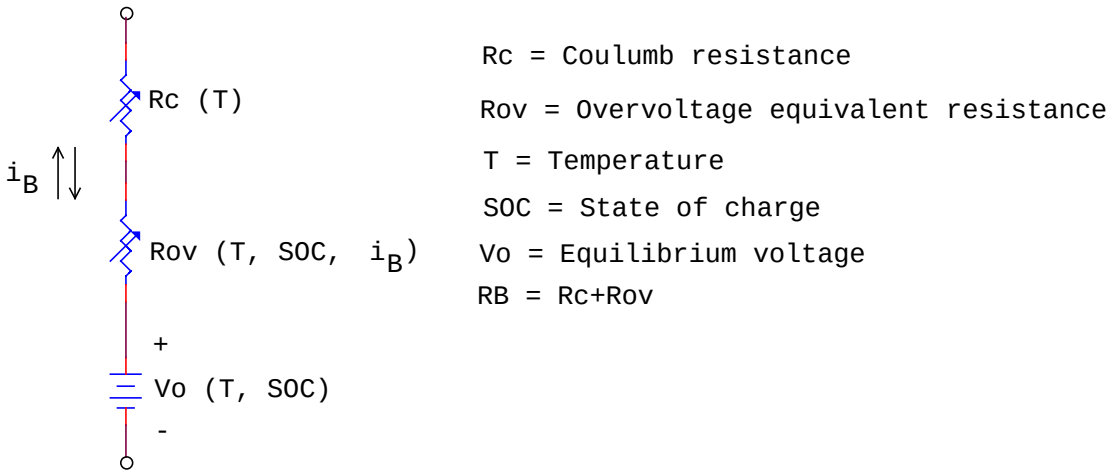

Fig. 1. Battery model.

2. A conventional coulomb resistance, R_c, that represents the ohmic voltage drop.
3. An equivalent resistance, R_{ov}, called the overvoltage resistance. This is explained below.

R_{ov} is not a resistance in the usual sense, but a component used to account for the extra energy that must be supplied to get charge into or out of V_0 [2,3]. As the battery temperature drops, R_{ov} increases because more energy is required to either charge or discharge the battery. R_{ov} is highly nonlinear with respect to the state of charge (SOC) and the magnitude and direction of the current, i_B.

At a sufficiently low temperature and SOC, R_{ov} becomes so large that the battery is virtually unusable. Assuming V_0 remains fairly constant, the detrimental effect of a large R_{ov} on discharge is obvious once R_{ov} begins to approach or exceed the load resistance. Also, a high R_{ov} seriously limits the charging ability of the battery. Because of the energy level required to force a higher current through a high R_{ov}, this also creates excessive gassing. This leads to a loss of electrolyte, and for sealed batteries the internal pressure can exceed the capacity of the relief valves. When this happens, it is quite easy to rupture the battery case. Therefore, use of DC currents for heating the electrolyte is not practical and can be extremely detrimental, especially for sealed batteries because at very low temperatures DC currents of even moderate amplitudes can create excessive gassing long before significant heating occurs. However, it will be shown that fairly high alternating current (AC) currents can be used to heat a battery, while avoiding these problems.

2. Battery heating methods

Batteries can be warmed by applying heat either externally or internally. There are several methods that could be used for external heating such as electrically heated thermal jackets, a sealed enclosure with an internal heating element, warm air heating, and liquid heating.

These methods typically use a separate power source for a heating element which provides the required energy. The resultant heat is then transferred to the battery by either a conduction or a convection system. While convection systems blow hot air across the battery, conduction systems apply heat directly to the battery surface. Obviously, each of these systems applies heat to the external surface of the battery, and a significant amount of heat is lost to the environment. Convection and conduction heating schemes also require an extensive mechanical structure located close to the batteries. Warm air heating and liquid heating also need mechanical systems that are fairly complex and use a substantial amount of power. A system using thermal jackets includes a flexible insulator that wraps around the exterior of the batteries with an externally powered heating element embedded on the inner surface of the insulator. While thermal jackets do not require complex mechanical systems they still need to be powered by an external power source.

In summary, all of these external heating methods add considerable weight and expense. Moreover, if the pack is allowed to reach a very low temperature, these methods require a significant amount of time for warming the batteries since the external heat energy must penetrate the large mass of the pack.

It would be much more beneficial to heat the battery electrolyte directly rather than using external heaters. As mentioned earlier, DC currents are not feasible for this purpose, but fairly high AC currents can indeed be used to provide heat via internal I^2R losses. This method has no effect on the cost of the pack itself, and it has been proven that it can heat a cold battery quite rapidly. This strategy does not require complex mechanical structures, but there obviously is some expense for the equipment that applies the AC to the battery.

AC can be circulated through the battery at either a low frequency, such as 60 Hz, or a high frequency of the order of 10–20 kHz [4]. The use of 60 Hz is economically attractive

because it is relatively simple and cheap as compared to higher frequency systems. However, the 60 Hz equipment is much larger and heavier. Therefore it would be a poor choice for on-board purposes and can be used only as an off-board heater. An on-board HEV heater, however, will require a high frequency heater to reduce size and weight. Energy for this inverter would be supplied by the on-board generator that is driven by the HEV's heat engine, i.e., it is not feasible for the battery to provide enough energy to heat itself.

To determine the effects of AC heating on HEV batteries at cold temperatures, both 60 Hz as well as 10–20 kHz heating were investigated in a comprehensive manner. Experimental set-ups were built for both frequencies, and several tests were conducted on both lead acid and NiMH batteries at different AC amplitudes, SOCs and cold temperatures. Sixty Hertzs heating was first tested for several lead acid batteries, and later the concept of using high frequency heating was verified by building and testing a 10–20 kHz inverter for nickel metal hydride (NiMH) batteries.

3. Battery charger with 60 Hz AC heater

Fig. 2 shows the test circuit of the system which uses a 60 Hz source to provide the AC current, along with a charger that is represented by the current source, I_{DC} [5]. This experimental set-up was used to observe whether the battery accepts charging current at cold temperatures as it warms up. The 60 Hz heating current, I_{AC}, is supplied from the source, V_s, via the current transformer, T. The inductance (L) was 5.76 mH, and the inductive reactance (X_L) at 60 Hz equaled 2.156 ohms. This value was sufficient to force virtually all of I_{AC} to flow through the battery since R_B is of the order of tens of milliohms so that $X_L \gg R_B$. The capacitor, C, was used to prevent I_{DC} from flowing through T.

The control system uses the input measurements T_B, V_B, I_{DC} and I_{AC}, to regulate I_{AC} and either I_{DC} or V_B, depending on whether current or voltage regulation is required. The control system also ensures that none of the limits are exceeded. A Crydom 10PCV2415 Power Controller was used for regulating I_{AC}. It consists of two back to back SCRs whose firing angles can be controlled. The firing of the SCRs was controlled by inputting a DC voltage in the range of 2–10 V to the Power Controller which controls the firing angle over the range of 0–180° for each SCR. A Phytec KitCON-505C evaluation board was used for programming an 8 bit Infineon C505C microcontroller for implementing the above tasks.

4. 10–20 kHz heating

The concept of using high frequency AC heating was verified by using a variable frequency 10–20 kHz inverter for tests on a pack of nickel metal hydride (NiMH) batteries. Experiments were conducted on 16 series connected Panasonic NiMH batteries (rated at 6.5 Ah) having a combined voltage of approximately 128 V. While other types of batteries such as lead–acid, NiCd, and Li-ion can be used for testing purposes, NiMH was chosen because it is currently used in certain HEVs such as the Toyota Prius and the Honda Insight.

Fig. 3 shows the 10–20 kHz circuit [4], where the battery pack is divided into two halves whose voltages are V_{B1} and V_{B2}. The circuit includes a pair of IGBTs Q_1 and Q_2 connected in a half bridge configuration. Anti-parallel diodes D_1 and D_2 also are connected in parallel with Q_1 and Q_2,

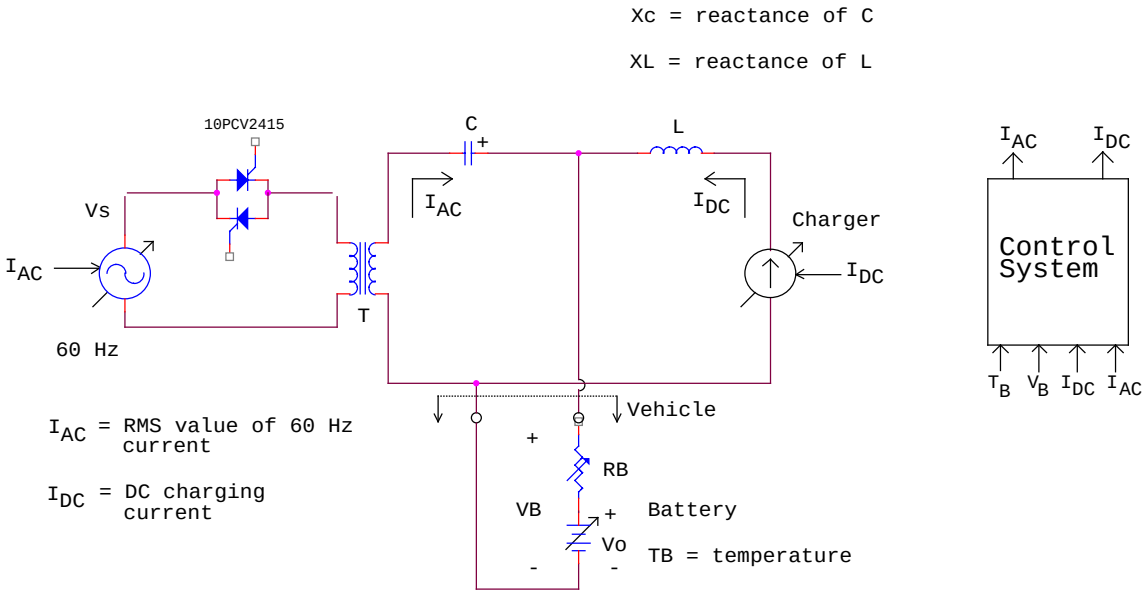

Fig. 2. Battery charger with 60 Hz. AC heater.

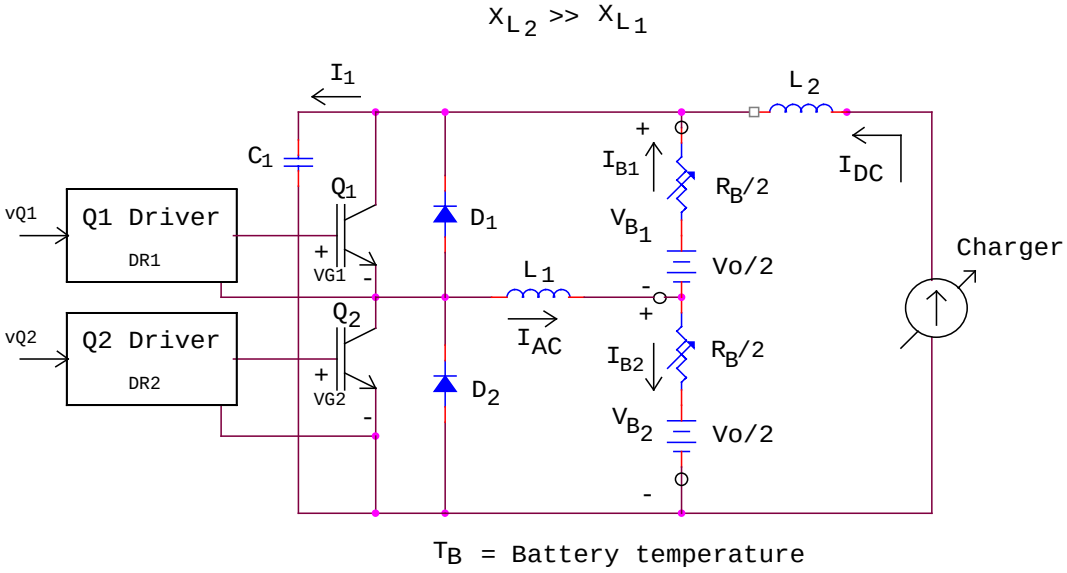

Fig. 3. Battery charger with 10–20 kHz. AC heater.

respectively. The circuit uses variable frequency modulation to control the current amplitude over a 10–20 kHz frequency range. This frequency range was selected to minimize the inductor weight and size without creating excessive losses in the inductor or the power semiconductors.

The purpose of this circuit is to circulate an AC current between the two halves of the pack. Therefore, each half is alternately charged and discharged and thus heated by internal $I^2R_B/2$ losses. This circuit provides the advantage of much smaller reactive components than the 60 Hz circuit, but it is also more complex and expensive because of the power electronics equipment.

In Fig. 3, a third connection is made to the center of the battery pack. Referring to the i_{AC} waveform in Fig. 4, the V_{G1} output from the Q_1 driver card (DR_1) turns transistor Q_1 ON at t_0. Since the voltage drops across $R_B/2$ and Q_1 are very small, the voltage from the top half of the pack, V_{B1}, is impressed across inductor L_1. Therefore i_{AC} starts increasing linearly with time, storing energy within L_1. At t_1, DR_1 drives V_{G1} to the low state. Transistor Q_1 then begins to turn OFF at t_1 and i_{AC} starts commutating through diode D_2. i_{AC} then flows in the D_2, L_1, V_{B2} loop until it reaches zero at t_2. In other words, the current which flows through L_1 begins to conduct through the lower half of the battery pack. Thus for $0 \le t \le t_1$, energy is removed from V_{B1} and stored in L_1. For $t_1 \le t \le t_2$, the energy in L_1 is transferred to V_{B2}.

At a time slightly before t_2, the Q_2 driver card (DR_2) drives V_{G2} high, turning Q_2 ON. It is observed that Q_2 turns ON while current flows through the anti-parallel diode D_2, resulting in virtually zero turn-on loss in Q_2. The turn-on losses for an IGBT are directly proportional to the square of the voltage from the collector to emitter. Normally the voltage from collector to emitter would be approximately 64 V for this circuit. However, by turning the IGBT ON while current is flowing through the anti-parallel diode, the collector to emitter voltage at turn-on is approximately one diode drop, which is less than 1 V. Therefore, turn-on losses of Q_2 are decreased dramatically.

Current in the anti-parallel diode D_2 continues to decrease until it reaches zero, at which time i_{AC} begins to flow into the collector of Q_2 and up through the lower half of the battery pack. As current flows through L_1, energy is transferred from the lower half of the pack into L_1 until Q_2 turns OFF. At time t_3, DR_2 drives V_{G2} low to turn Q_2 OFF. As Q_2 turns OFF, the current flowing through the inductor begins to flow up through the anti-parallel diode D_1 and down through the top half of the pack, i.e., the D_1, V_{B1}, L_1 loop. The voltage from the batteries is impressed across L_1 causing current i_{AC} to decrease linearly. During this period energy is transferred from L_1 into the top half of the pack. At some time prior to i_{AC} reaching zero, Q_1 is turned ON, thereby attaining virtually lossless turn-on in a manner similar to Q_2. When i_{AC} becomes zero, diode D_1 becomes back-biased and i_{AC} once again flows through the Q_1, L_1, V_{B1} loop. The waveforms for i_{AC}, i_{Q1}, i_{Q2}, i_{D1}, i_{D2}, V_{G1}, and V_{G2} are shown in Fig. 4.

Therefore energy is cycled between the two halves of the pack, which means that the AC RMS battery current in either the $Q_1 - D_1$ or the $Q_2 - D_2$ branch is $I_{AC}/\sqrt{2}$. Referring to Fig. 3 L_2 is chosen so that $X_{L2} \gg X_{L1}$. This insures that I_{DC} remains essentially constant, and virtually no 10–20 kHz current flows through the charger. C_1 is used in Fig. 3 to prevent excessive voltage transients across Q_1

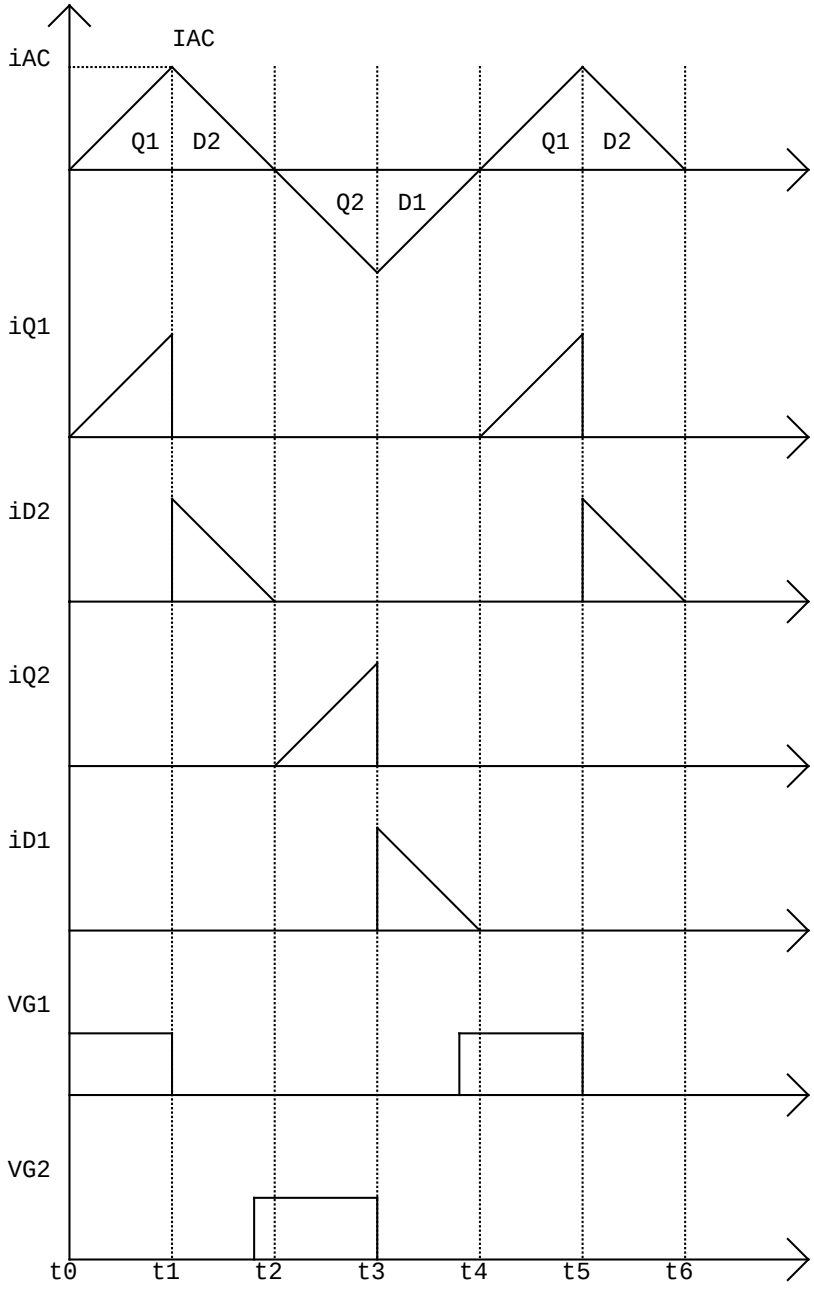

Fig. 4. i_{AC}, i_{Q1}, i_{Q2}, i_{D1}, i_{D2}, V_{G1}, and V_{G2} waveforms for the circuit in Fig. 3.

and Q_2 when they turn OFF. While C_1 must be large enough to provide protection, it also should be as small as possible to minimize I_1. This is because I_1 represents current that is siphoned away from I_{B1} and I_{B2}. To avoid overheating, a polypropolene capacitor was used for C_1. If $C_1 = 0$, then $I_{B1} = I_{B2} = 0.707\ I_{AC}$, in which case the AC conduction losses in the pack are

$$2\left(\frac{I_{AC}}{\sqrt{2}}\right)^2 \frac{R_B}{2} = \frac{{I_{AC}}^2 R_B}{2} \tag{3}$$

Therefore in order to achieve $I_{B1} = 100$ A rms, for this ideal case we would need $I_{AC} \cong 141.4$ A rms. In the actual circuit C_1 was 20 μF, and I_{B1} was somewhat less than 100 A rms when $I_{AC} \cong 141.4$ A rms because of the C_1 siphoning effect. This occurs because of fairly complex resonant effects between C_1 and other reactances, and as a result, the actual I_{B1} is difficult to calculate exactly and must be measured.

5. Experimental results for low frequency (60 Hz) heating

One area of interest was to produce a test that would emulate the starting condition of a vehicle. This was done

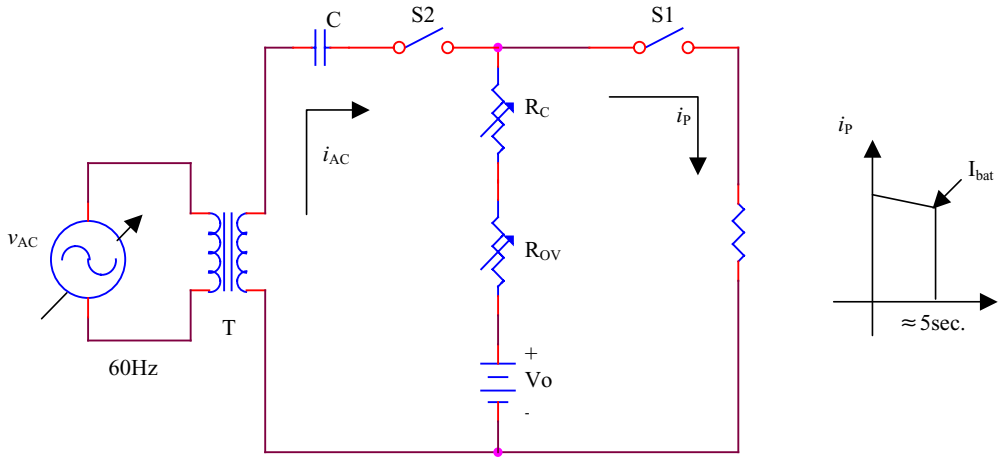

Fig. 5. Pulse discharge test circuit.

by measuring the amplitude of the current pulse that occurs when a very low resistance load is applied for 5 s. If only a few pulses are applied, e.g., less than 4 or 5, these pulses are also short enough to have only a minor effect on the SOC. The simplified schematic is shown in Fig. 5. This set up was used for testing one 12 V lead acid battery module. During a pulse test, S_2 was open and S_1 was momentarily closed, allowing current to flow through the low resistance for at least 5 s. The pulse amplitude at 5 s (I_{bat}) obtained by this method gives a reasonable estimate of the battery performance at different temperatures.

Tests were conducted on a Hawker Odyssey PC1200 battery. The battery SOC was set to be approximately 50%. Referring to Fig. 5, a very low resistance load was applied across the battery by closing switch S_1 for slightly over 5 s. In the first test at 25 °C, switch S_2 was left open (no AC), and the pulse amplitude at $t = 5$ s. was observed to be 250 A (Fig. 6). The battery was then soaked at −40 °C for more than 10 h and re-tested without AC. Fig. 7 shows that the amplitude at $t = 5$ s. decreased to ≅45 A. S_2 was then closed for 5 min (S_1 open) and 100 A rms was applied to the battery at 60 Hz. S_2 was then opened and S_1 was closed for about 5 s. The result obtained is shown in Fig. 8. The amplitude of the pulse discharge increased to ≅140 A. The AC power dissipation in the battery after 5 min (S_1 open, S_2 closed)

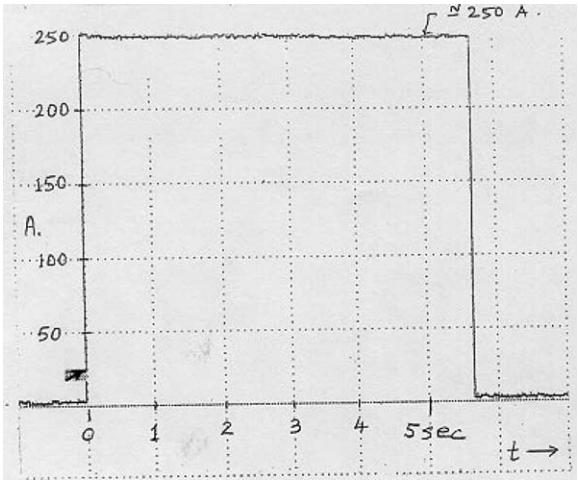

Fig. 6. Pulse discharge current at 25 °C, SOC ≅ 50%.

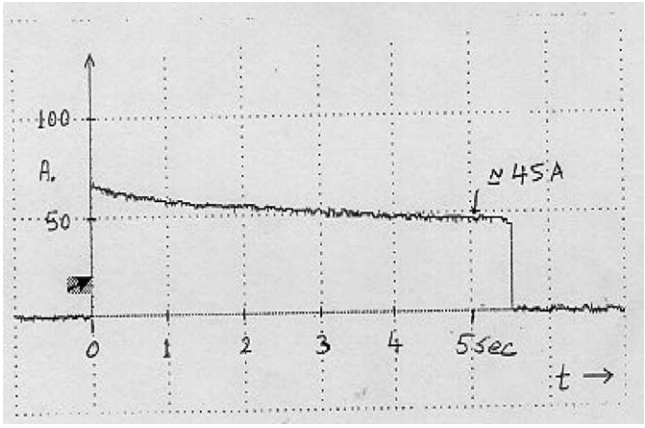

Fig. 7. Pulse discharge current at −40 °C, SOC ≅ 50% before AC heating.

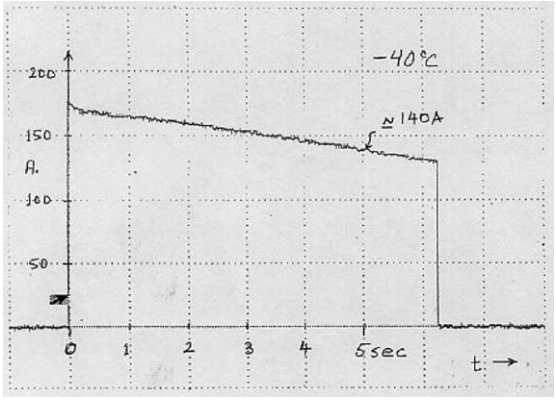

Fig. 8. Pulse discharge current at −40 °C, SOC ≅ 50% after $I_{ac} = 100$ A rms for 5 min.

Table 1
Hundred ampere rms results

Temperature (°C)	AC period (min)	P_{AC} (W)	I at 5 s (A)
25	0	–	250
25	5	43	–
−40	0	–	45
−40	5	239	140
−40	10	180	140
−40	15	152	145

was 239 W. In another test, when AC current was applied at 25 °C for 5 min, the AC power was only 43 W at 100 A rms. This indicates that R_B at −40 °C increased by a factor of approximately 5.6. Additional tests were performed at −40 °C after 100 A rms was applied for 10 and 15 min. The results are summarized in Table 1.

These results therefore indicate that a 100 A rms AC current at −40 °C was able to revive a virtually unusable battery within 5 min. P_{AC} continues to decrease at the 10 and 15 min intervals due to heating of the electrolyte and thus lower R_B, but the pulse increase is negligible.

6. Effect of AC heating on battery charging ability

The circuit described in Fig. 2 was used to study the effect of AC heating on battery charging ability. Tests were carried out on a Hawker Odyssey PC1200 battery. As explained earlier, at lower temperatures, higher DC voltages are required to force DC currents through the higher R_B. However, if V_B is too high, excessive gassing can damage the battery. The charger voltage limit was therefore set at $V_B = 18$ V and its current limit at $I_{DC} = 40$ A maximum.

Fig. 9 shows the results of a charging test that was performed after soaking the battery for more than 12 h at −20 °C at SOC ≅ 50%. With no AC, at $t = 0$ the voltage limit of $V_B = 18$ V. was reached at only $I_{DC} \cong 2.5$ A. AC current was then applied, and the allowable I_{DC} increased as shown in Fig. 9. 100 A rms AC amplitude could not be reached immediately because the maximum available AC voltage was not high enough to force 100 A rms current through the high R_B. As R_B dropped, 100 A rms was reached at $t = 2$ min, and it was then held at that level until $t = 10$ min. With $V_B = 18$ V. limit the charger was able to reach $I_{DC} = 40$ A after 4 min. P_{AC} measurements over $3 \leq t \leq 10$ min. show a rapid drop because of the decrease in R_B as the battery electrolyte warms. For $t \geq 4$ min, the charger is in the current limit mode at $I_{DC} = 40$ A. and V_B decreases slowly, although this is not shown on the graph. Above $t \geq 11$ min, I_{AC} was progressively decreased just enough to keep I_{DC} fixed at 40 A. This is possible because the electrolyte has warmed up, and less heat is required to maintain the necessary temperature to hold I_{DC} at 40 A for $V_B \leq 18$ V. After $t \geq 21$ min it was possible to maintain $I_{DC} = 40$ A without any AC.

The above results therefore show that it is possible to charge a lead acid battery at cold temperatures with simultaneous AC heating. As stated earlier however, the use of only DC currents for heating the electrolyte is not feasible. This was verified by performing a test on a Hawker Odyssey PC1200 battery at SOC ≅ 40%. In order to provide about the same input power as in one of the previous AC tests, it was decided to circulate a DC current of about 11 A for heating the electrolyte. The pulse amplitude was first measured at room temperature and was observed to be 250 A at $t = 5$ s (Fig. 10). The battery was then soaked at −40 °C for 10 h and a pulse test was performed. Fig. 11 shows that the amplitude decreased to ≅45 A at $t = 5$ s. DC current of 11 A was then applied to the battery for 15 min. After 15 min another pulse test was performed. The result obtained is shown

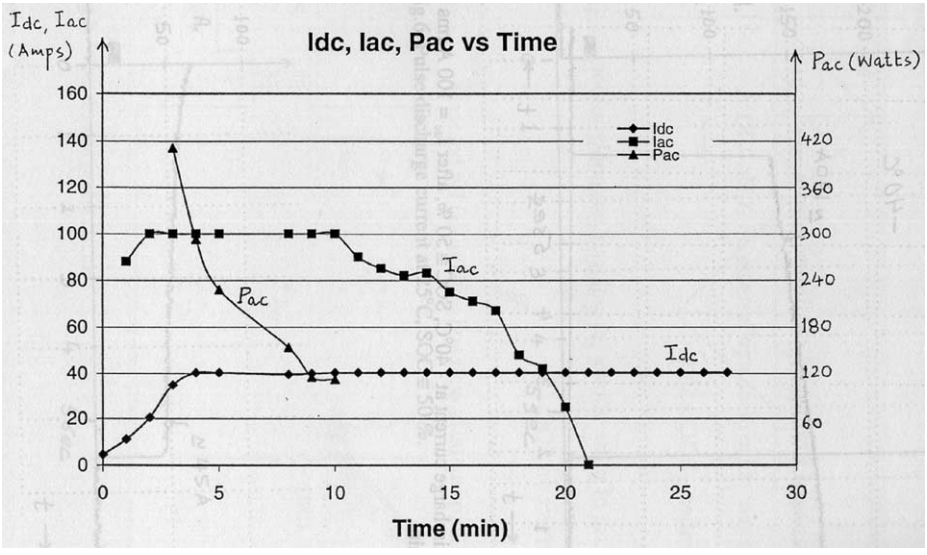

Fig. 9. Charging with AC heating vs. time for −20 °C.

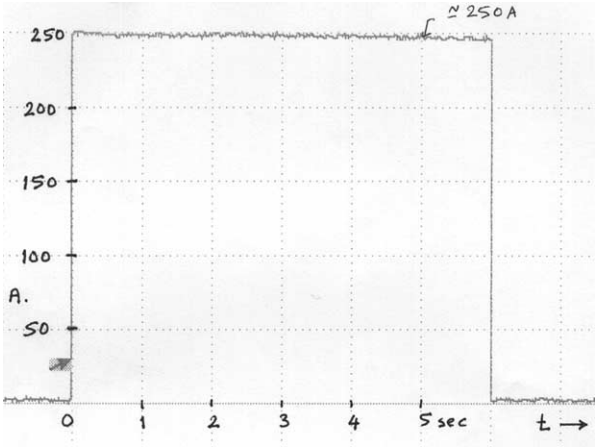

Fig. 10. Pulse discharge current at 25 °C, SOC ≅ 40%.

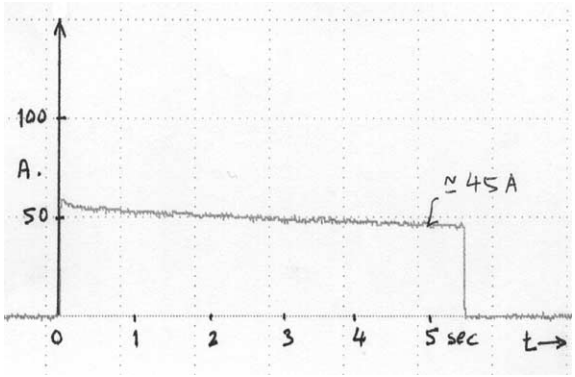

Fig. 11. Pulse discharge current at −40 °C, SOC ≅ 40% before DC heating.

in Fig. 12 where the amplitude of the pulse discharge increased to ≅65 A. Although the pulse current increased from 45 to 65 A in 15 min, a voltage of 22 V was required by the charger to provide the 11 A DC current. This led to severe gassing which ruptured the plastic battery case during this test. Thus, DC currents of even moderate amplitudes are extremely detrimental, especially for sealed batteries because they create excessive gassing long before significant heating occurs.

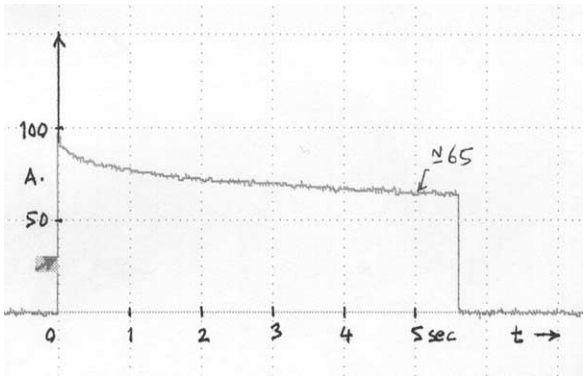

Fig. 12. Pulse discharge current at −40 °C, SOC ≅ 40% after $I_{DC} = 11$ A for 15 min.

Although 60 Hz heating can improve performance, some battery experts have indicated that each 8.33×10^{-3} s. half cycle is also time enough for significant ionization to occur. This indicates that 60 Hz current would decrease the battery lifetime. However at frequencies above 10 kHz, no one has yet indicated to the authors that a half cycle of no more than 50×10^{-6} s. would be detrimental, and test results on heating effects in this higher frequency range are presented in the next section. Although no ill effects were observed during these 10 kHz tests, the overall effect on battery lifetime may deserve more attention. An in-depth analysis of the battery chemistry and/or extended life tests might be useful areas for further study.

7. Experimental results for high frequency (10–20 kHz) heating

After the 60 Hz experiments were complete, a 10–20 kHz inverter was used to conduct heating tests on a pack of 16 series connected 6.5 Ah Panasonic NiMH battery modules. The nominal open battery circuit voltage was about 8 V per module at 25 °C over most of the SOC range. To measure internal battery temperature, the battery resistance series, R_B, was first measured after the battery was soaked for several hours at various temperatures. Fig. 13 shows the pulse profile [6] used to measure R_B. The pulses were generated using an AeroVironment ABC-150 power processing system along with its remote operating software (ROS) and a personal computer. Data acquisition was performed using a National Instruments PCI-6024E NI-DAQ card that interfaced with a 16 channel Analog Devices 5B Series signal conditioning module. Eight channels were used for measuring battery voltages and the remaining eight were used to sense the module temperatures. R_B was calculated as follows:

$\Delta V_0 = V_0$ voltage drop (during the discharge cycle)

when the I_0 pulse is applied; $\qquad R_B = \dfrac{\Delta V_0}{I_0}$.

It should be noted that the charger in Fig. 3 must supply the losses in both the battery pack and the AC heating circuit

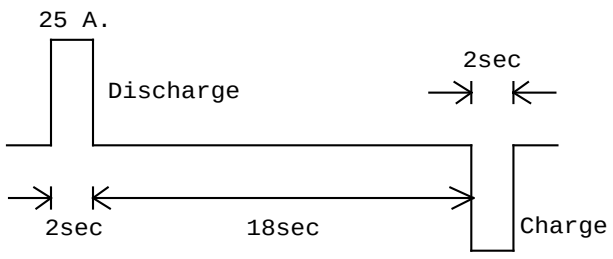

Fig. 13. I_0 characterization profile.

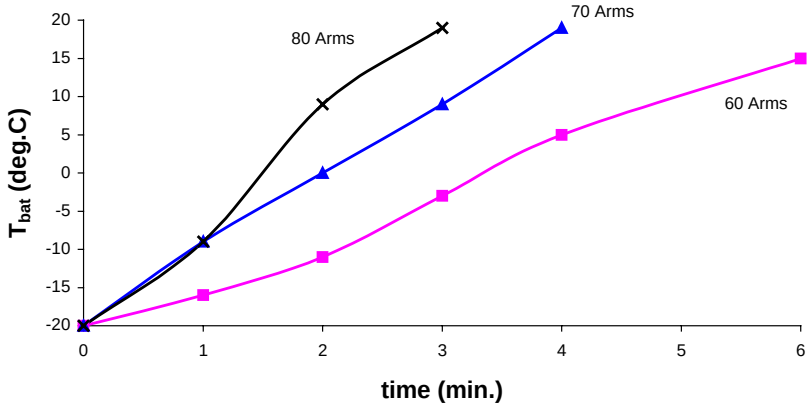

Fig. 14. T_{bat} vs. time at −20 °C, SOC ≅ 55%.

to prevent significant battery discharge. During the tests the charger was set in the voltage regulation mode in order to fulfill this task.

Test results in Figs. 14 and 15 at −20 °C and SOC = 55% show that it is possible to heat the pack close to room temperature within about 6–8 min by circulating a 10–20 kHz 60 Arms AC current [7]. However, a time lag of even 6 min may be unacceptable for HEV applications. Therefore, the effects of higher AC amplitudes were also studied. Tests at different temperatures and SOCs also were conducted to determine the effects of these variables.

To speed up the heating process, AC currents at amplitudes above 60 Arms were next circulated through the pack. Figs. 14 and 15 also show these results after soaking the battery pack for at least 5 h at −20 °C with an SOC ≅ 55%. Before applying the AC, R_B ≅ 1 ohm and T_{bat} ≅ −20 °C. T_{bat} then increased to about 15 °C and R_B decreased to about 0.3 ohm after 6 min of 60 Arms AC circulation. As expected, when the amplitude of AC was increased the heating process sped up. With 70 Arms AC circulation, 4 min were needed to heat the pack to about 18 °C, and with 80 Arms, only 3 min were needed.

Figs. 16 and 17 show the results obtained after soaking the battery pack for 5 h at −30 °C with an SOC ≅ 55%. Before applying the AC, R_B ≅ 1.3 ohm and T_{bat} ≅ −30 °C. T_{bat} then increased to about 14 °C and R_B decreased to about

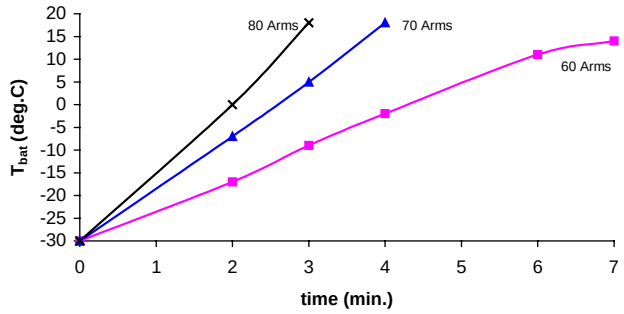

Fig. 16. T_{bat} vs. time at −30 °C, SOC ≅ 55%.

0.3 Ω after 7 min of 60 Arms AC circulation. However, the results for 70 and 80 Arms were about the same as those for −20 °C, e.g., with 70 Arms AC circulation, 4 min were needed to heat the pack to about 18 °C, and with 80 Arms, 3 min were needed.

In order to observe the effects of AC heating at different SOCs, tests were conducted at SOCs of 25, 55, and 75% using AC at an amplitude of 60 Arms. Figs. 18 and 19 show the results obtained after soaking the pack for 5 h at −30 °C and circulating 60 Arms with SOCs of 25, 55, and 75%. In this case, about 6 min were needed to heat the pack to about 15 °C when the pack SOC was 75%, but more time was

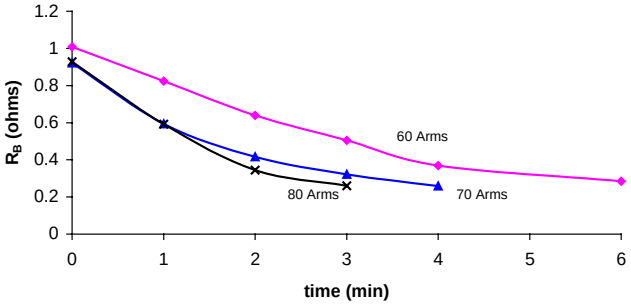

Fig. 15. R_B vs. time at −20 °C, SOC ≅ 55%.

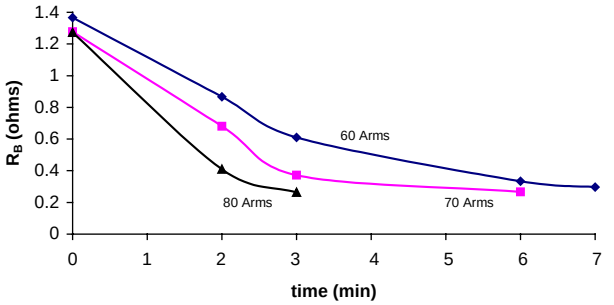

Fig. 17. R_B vs. time at −30 °C, SOC ≅ 55%.

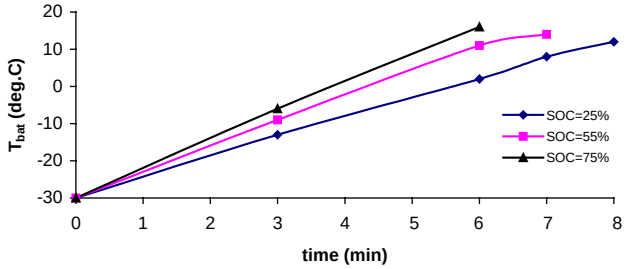

Fig. 18. T_{bat} vs. time at −30 °C, 60 A rms.

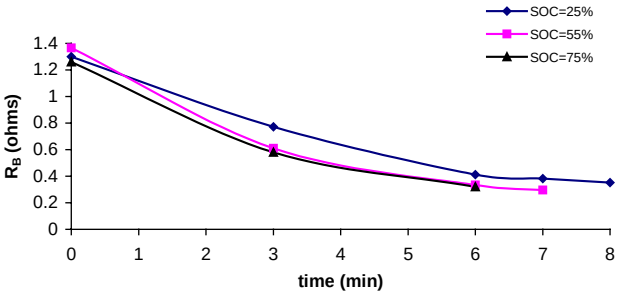

Fig. 19. R_B vs. time at −30 °C, 60 A rms.

needed when the SOC was lower. As shown by the plots for SOC = 55%, T_{bat} was about 13 °C after 7 min, and for SOC = 25% T_{bat} was about 12 °C after 8 min. This indicates that for colder temperatures the SOC does have some effect on the heating time.

To determine if 10–20 kHz heating improved the discharge capability of the NiMH pack at cold temperatures, discharge tests also were conducted using the ABC-150. The results obtained at −20 °C are shown in Fig. 20. Tests were conducted at three SOCs viz. 25, 55, and 75%. At SOC = 25%, the discharge Ah doubled from 0.45 to 0.9 Ah after 6 min of 60 Arms heating. At SOC = 55%, the discharge Ah improved from 1.99 to 2.84 Ah, an increase of 43%. Similarly, there was an improvement of about 17% at SOC = 75%. The results were more prominent at −30 °C, as shown in Fig. 21. At SOC = 25%, the discharge Ah without AC equaled 0.3 Ah and improved to 0.95 Ah after 6 min of 60 Arms heating. At SOC = 55%, the discharge Ah improved from 0.5 to 2.59 Ah, an increase of more than 5 times. At SOC = 75%, the discharge Ah without AC equaled 0.75 Ah, and it increased to 3.58 Ah after 6 min of AC circulation.

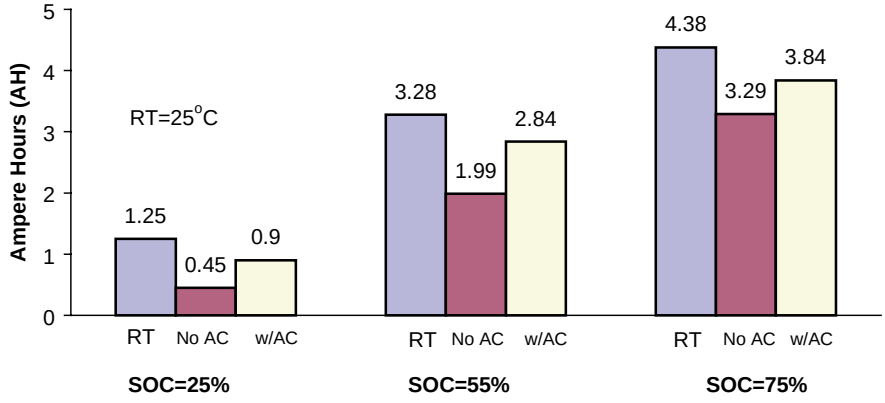

Fig. 20. Discharge tests at −20 °C.

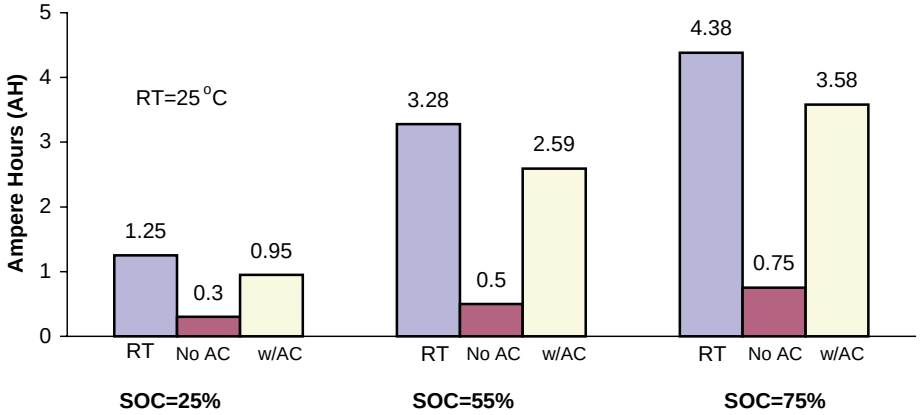

Fig. 21. Discharge tests at −30 °C.

8. Conclusions

Several tests were initially conducted to measure the effect of 60 Hz AC heating on different lead acid batteries. It was decided to test 60 Hz heating first because it is readily available in stationary applications. In order to simulate the starting condition of a vehicle, the amplitude of a high current pulse was measured by applying a very low resistance load for slightly over 5 s. Several tests were conducted at different SOCs and at cold temperatures in the −20 °C to −40 °C range. Although 50–60 A rms AC heating proved beneficial, these currents took an excessive amount of time before adequate heating results were observed. However, the required heating time was easily decreased by increasing the AC current amplitude. With 100 A rms AC heating a virtually unusable lead acid battery was revived within 5 min.

After verifying AC heating at 60 Hz, high frequency heating was tested using a 10–20 kHz inverter on a pack of 16 series connected Panasonic NiMH batteries. The test conditions were designed to simulate those on an HEV where a generator would be available to replace the energy lost in the heating process. Several tests were conducted to investigate the effects of different SOCs and cold temperatures. These tests show that at both −20 and −30 °C, 10–20 kHz AC currents at amplitudes of 60–80 A rms can restore the battery resistance and temperature to values close to those at 25 °C within a few minutes. As expected, the heating process sped up as the amplitudes of the AC was increased. It is also evident that while operating the AC heater, it is necessary to simultaneously use a DC generator (charger) to replace the heating losses or rapid discharge will occur.

Acknowledgements

This research was supported by grants from Daimler-Chrysler, AG and the US Department of Energy National Renewable Energy Laboratory (NREL) under grant no. ACI-9-29118-01. The authors would also like to acknowledge the advice and assistance provided by Dr. Cyrus Ashtiani from DaimlerChrysler and Dr. Ahmad Pesaran and Mr. Mathew Keyser from NREL.

References

[1] D. Linden, Handbook of Batteries and Fuel Cells, McGraw-Hill, 1995.
[2] D. Berndt, Maintenance-Free Batteries, second ed., Research Studies Press Ltd., Taunton, England, 1997.
[3] D. Rand, R. Woods, R. Dell, Batteries for Electric Vehicles, Research Studies Press Ltd., Taunton, England, 1998.
[4] C. Ashtiani, T. Stuart, Circulating Current Battery Heater, US Patent 6,259,229 (10 July 2001).
[5] T. Stuart, A. Hande, AC battery heating for cold climates, in: Proceedings of the EnV 2001 Conference, Engineering Society of Detroit, Southfield, MI, 10–13 June 2001.
[6] PNGV Battery Test Manual, US Department of Energy, DOE/ID-10597, Revision 3, February 2001.
[7] T. Stuart, A. Hande, AC heating for EV/HEV batteries, in: Proceedings of the 7th IEEE Workshop on Power Electronics in Transportation (WPET 2002) Conference, Detroit, MI, 24–25 October 2002.